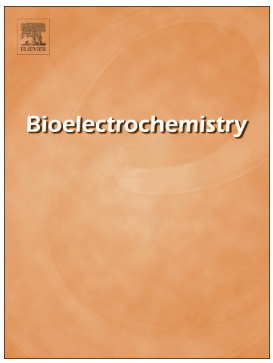

Acetylcholinesterase modified AuNPs-MoS2-rGO/PI flexible film biosensor: Towards efficient fabrication and application in paraoxon detection

Lingpu Jia, Yaxin Zhou, Kaipeng Wu, Qingling Feng, Chunming Wang, Ping He

PII: S1567-5394(19)30332-9

DOI: https://doi.org/10.1016/j.bioelechem.2019.107392

Reference: BIOJEC 107392

To appear in: *Bioelectrochemistry*

Received date: 2 June 2019

Revised date: 9 September 2019

Accepted date: 10 September 2019

Please cite this article as: L. Jia, Y. Zhou, K. Wu, et al., Acetylcholinesterase modified AuNPs-MoS2-rGO/PI flexible film biosensor: Towards efficient fabrication and application in paraoxon detection, *Bioelectrochemistry* (2018), https://doi.org/10.1016/j.bioelechem.2019.107392

Acetylcholinesterase modified AuNPs-MoS_2-rGO/PI flexible film biosensor: Towards efficient fabrication and application in paraoxon detection

Lingpu Jia[a*], Yaxin Zhou[b], Kaipeng Wu[a], Qingling Feng[c], Chunming Wang[b], Ping He[a]

a State Key Laboratory of Environment-friendly Energy Materials & School of Materials Science and Engineering, Southwest University of Science and Technology, Mianyang 621010, China
E-mail: jialp@lzu.edu.cn
b Lanzhou Institute of Husbandry and Pharmaceutical Sciences of CAAS, Lanzhou 730000, China
c Shaanxi Key Laboratory of Optical Information Technology, School of Science, Northwestern Polytechnical University, Xi'an 710129, China

Abstract

A flexible acetylcholinesterase (AChE) film biosensor, based on a AuNPs-MoS_2-reduced graphene oxide/polyimide flexible film (rGO/PI) electrode, has been synthesized for paraoxon detection. In this study, the rGO/PI film acts as the flexible substrate and AuNPs are reduced by monolayer MoS_2 under illumination. Transmission electron microscopy revealed that AuNPs are uniformly dispersed on the MoS_2-rGO/PI electrode surface with a diameter ~10 nm. X-ray photoelectron spectroscopy indicated that a strong binding force exists between reduced AuNPs and monolayer MoS_2. The AChE modified AuNPs-MoS_2-rGO/PI flexible film biosensor is used to hydrolyze acetylcholine chloride and obtain a large current response at 0.49 V by differential pulse voltammetry, demonstrating successful immobilization of AChE. In view of the inhibition of paraoxon on the AChE, under optimal conditions, the AChE/AuNPs-MoS_2-rGO/PI film biosensor shows a linear response over a concentration range 0.005–0.150 μg/mL, a sensitivity of 4.44 uA/μg mL^{-1}, a detection limit of 0.0014 μg/mL, acceptable reproducibility and stability to paraoxon. The flexible film biosensor has also proved used for detection of paraoxon in real samples.

Keywords: Photo-reduction, Flexible film, AuNPs/ MoS_2, AChE, Pesticide

1. Introduction

Organophosphorus pesticides (OPs) are known as toxic agricultural wastes, and they are widely used in increasing agricultural productivity. But the long-term accumulations can cause serious damage to human health as they irreversibly inhibit the catalytic activity of acetylcholinesterase (AChE) [1-4]. Therefore, in order to protect humans from the risk of pesticides in environmental water and food, it is of great significance to develop a fast and reliable analytical method for pesticide detection at very low concentration levels [5, 6].

One of the most promising research in this area is related to AChE biosensors [7-9]. First of all, it has fast response and high sensitivity [10]. Secondly, the combine nanostructure with enzyme has opened a new route in enzyme engineering [11, 12]. Therefore, numerous biosensors based on AChE have been developed for environmental monitoring, toxicity analysis and food quality control in recent years [13, 14]. For enzyme sensors, efficient immobilization of the enzyme on the electrode surface with maintaining its native catalytic activity is the key issue [15]. The existing immobilization methods include direct physical adsorption, physical entrapment in polymers or sol-gels and self assembling, but they are usually immobilized on glassy carbon modification electrode rather than flexible film electrode [16, 17]. So far, more and more researchers have shifted their attention to fabricate flexible electrode owing to its advantages in flexibility, lightweight, low cost and high surface area, which has been utilized widely in supercapacitor and battery [18, 19].

Reduced graphene oxide/polyimide (rGO/PI) composite electrode is a class of conductive composite film electrode, consisted of rGO and PI. rGO as a nanometer carbon material exhibits rapid electron transfer kinetics, mechanical property and large specific surface area. PI is a polymer with good film forming property. The perfect combination between rGO and PI not only develops excellent electrical conductivity, mechanical property, flexibility and temperature tolerance [20-23], but also possesses wide potential range. So the rGO/PI film is a new potential flexible film electrode [24, 25].

It is known that AuNPs serve as one of most stable metal nanoparticles, have been widely applied in enzyme sensor for its strong Au-S bond effect, novel electrical, catalytic properties and good biocompatibility [26-28], and it is also employed to immobilize AChE in this work. Monolayer MoS_2 is a direct band gap semiconductor with 1.8 eV [29], which particularly attracts attentions for photoelectric property, solar spectrum absorption, high specific surface area and relatively high carrier mobility. In most researches, AuNPs are usually coated on electrode surface and could easily fall off in the process of measurement. In this work, AuNPs are directly reduced on the monolayer MoS_2 modified rGO/PI flexible film under illumination, which overcomes above deficiency. The formed AuNPs-MoS_2-rGO/PI flexible film is used to construct AChE biosensor and shows good performance for paraoxon, illustrating the AuNPs-MoS_2-rGO/PI flexible film is promising to be candidate in detecting organophosphorus pesticides.

2. Material and methods

2.1 Materials and Instruments

Monolayer MoS_2 was purchased from XFNANO company (nanjing, china), $HAuCl_4$ was obtained from Aladdin industrial corporation (Shanghai, China), Acetylcholinesterase (500 UN) and acetylcholine chloride (ATCh) came from Sigma, paraoxon was belong to J&K Scientific. The other regents were of analytical grade and were used without further purification.

All electrochemical experiments were performed on CHI 832 Instruments (CH Instrument, USA). All Characteristics were achieved by field-emission scanning electron microscope (FE-SEM) (Hitachi S-4800, Japan), transmission electron microscopy (TEM) (FEI Tecnai G^2 F30), high-resolution transmission electron microscopy (HRTEM), X-ray diffraction (XRD) (RigakuD/max-2400) and X-ray photoelectron spectroscopy (XPS). The xenon lamp (CHF-XM-500W, Beijing Trusttech Co.Ltd.) offered the light source.

2.2 Fabrication of rGO/PI flexible film electrode

The rGO/PI flexible film acts as the working electrode with the geometric area of 0.1256 cm^2, synthesized according to our previous work [30]. The mass ratio of rGO/PI is 15%. A Pt wire and a saturated calomel electrode correspond to counter and reference electrode, respectively. In order to strip the rGO/PI composite film from indium tin oxide (ITO) substrate, the rGO/PI-ITO was immersed in 5 M KOH solution, then dried at room temperature after washing with deionized water.

2.3 Construction of AChE/AuNPs-MoS_2-rGO/PI biosensor

The procedures for the preparation of AuNPs-MoS_2-rGO/PI biosensor are shown in Schematic 1. Firstly, 100 ul (0.015 mg/mL) ethanol dispersion solution of monolayer MoS_2 was dropped on rGO/PI flexible film electrode to form MoS_2 modified rGO/PI flexible electrode (MoS_2-rGO/PI) after dring at room temperature. Secondly, MoS_2-rGO/PI flexible electrode was immersed in 10 mL 0.300 mg/mL $HAuCl_4$ aqueous solution for 20 min under illumination, and then washed thoroughly with deionized water to remove unreduced Au^{3+}. Monolayer MoS_2 has 1.8 eV direct bandgap, and the $AuCl_4^-$ will capture the electron that valence band jumped into conduction band to form AuNPs when it is illuminated. Thirdly, the obtained AuNPs-MoS_2-rGO/PI film was soaked in 0.1 M phosphate buffer solution (PBS, pH 7.4) with 0.051 mg/mL AChE and stored in refrigerator at 4℃ for 24 h. Because of the specific strong interaction between AuNPs and S, the stability of AChE/AuNPs-MoS_2-rGO/PI film sensor is further improved. The film biosensor should be washed with PBS before measuring.

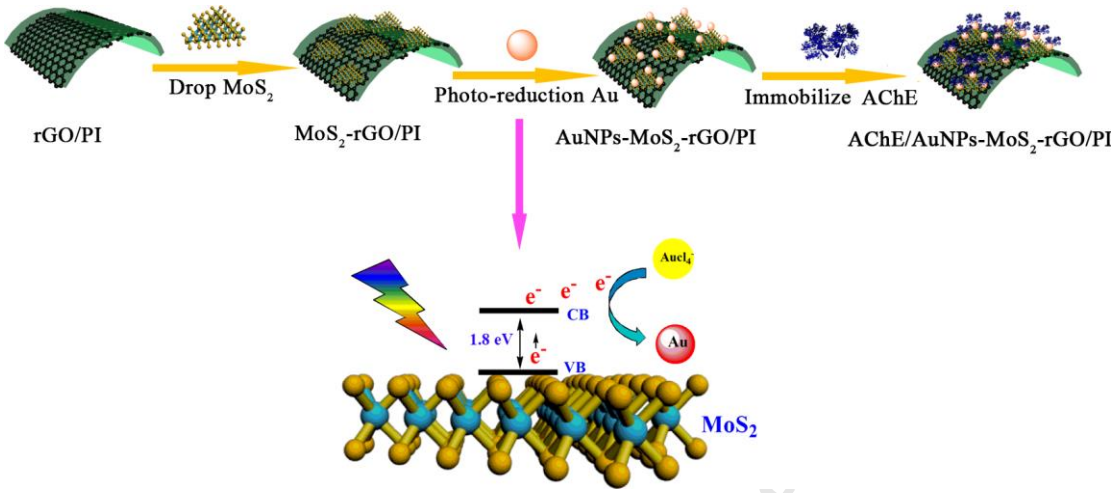

Schematic 1 Fabrication processes of AChE/AuNPs-MoS_2-rGO/PI flexible modified electrode and the reduction mechanism of AuNPs.

3. Results and Discussion

3.1 Characterizations

The morphology of rGO/PI film was investigated in detail by SEM. Shown in figure 1a is a cross-section image, and it is clear that rGO uniformly dispersed in PI film. For the enlarged view of figure 1b, one can even observe the typical layer morphology of rGO. These results indicate rGO and PI can form homogeneous flexible film without agglomeration, which not only provides a large specific surface area and more active sites but also retains good electrical conductivity of rGO. Figure 1c-d show the rGO/PI flexible film is 11 um in thickness with the size of 1cm ×1 cm.

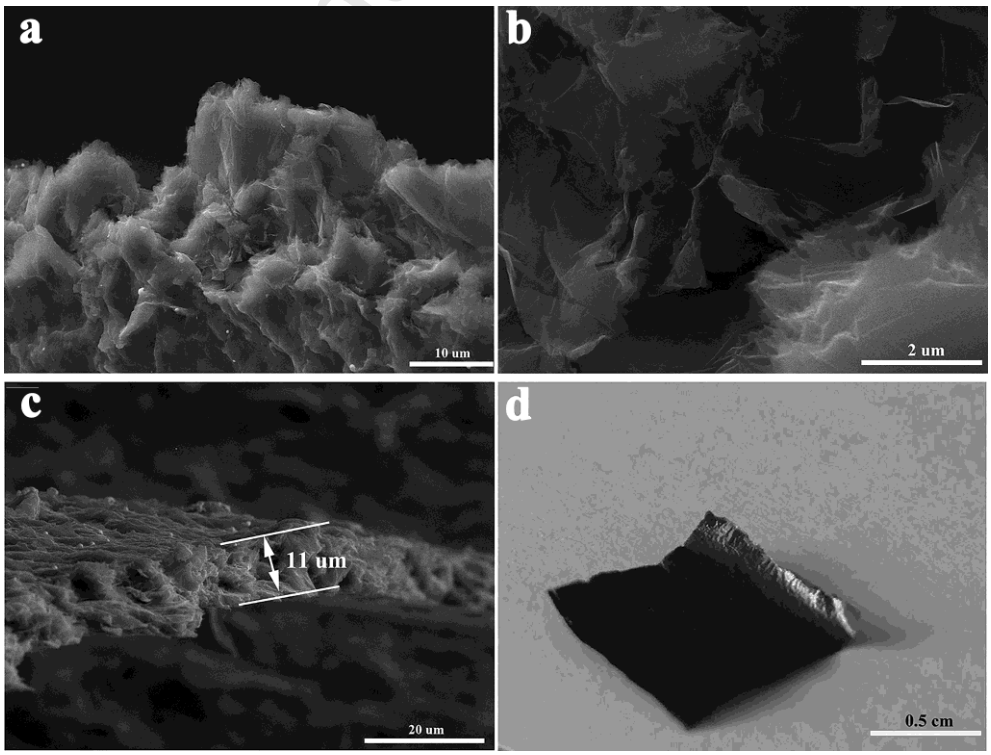

Figure 1 SEM of rGO/PI (a) cross-section, (b) cross-section enlarged, (c) thickness, (d) the picture of rGO/PI film.

TEM and HRTEM display the structure of AuNPs-MoS_2-rGO/PI film. Uniform AuNPs (Figure 2a) can be find on the momolayer MoS_2 surface. Figure 2b shows that the diameter of AuNPs is 10 nm, and it is much smaller compared with previous publications [31, 32]. It can also observe a lattice spacing of 0.232 nm, corresponding to the (111) plane of AuNPs. To further confirm the structure of AuNPs, the sample was researched by selected area electron diffraction(SAED) and XRD. As shown in figure 2c, there are five diffraction rings, and the diffraction ring for (111) plane seems much brighter than others, demonstrating the preferential crystal growth of AuNPs along the (111) plane. Figure 2d reveals the XRD results of obtained flexible films. The broad strong diffraction peak at 24° comes from rGO (curve a). Aside from diffraction peaks of MoS_2 (curve b), the rest of four diffraction peaks in curve c could be indicated to the crystal planes (111), (200), (220) and (311) of AuNPs, which matched with the hexagonal structure of Au (JCPDS 65-8601). The worth noting is that the (111) diffraction peak also exhibits the highest intensity, indicating the preferential growth of (111) plane. This is consistent with the result of SAED pattern.

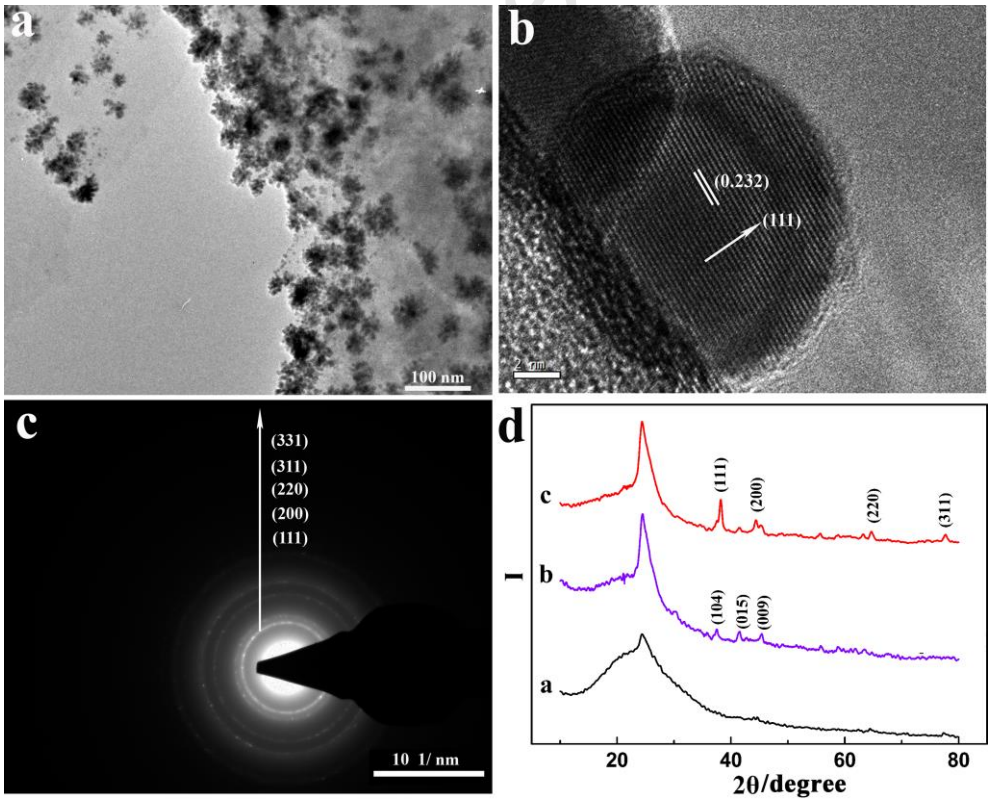

Figure 2 (a) TEM image of AuNPs modified monolayer MoS_2. (b-c) HRTEM and selected area electron diffraction images of AuNPs. (d) XRD patterns of rGO/PI (curve a), MoS_2-rGO/PI(curve b), and AuNPs-MoS_2-rGO/PI flexible film(curve c).

In order to gain more insight on the chemical state and the surface compositions of AuNPs-MoS_2-rGO/PI composite film, XPS technique studied the film, as shown in figure 3. The wide scan survey reveals that the sample contains the elements of Au, S, Mo, C, N and O (figure 3a). It is clear that S and Mo elements belong to monolayer MoS_2 (figure 3b-c), and C, N and O elements come from the substrate rGO/PI. Two peaks at 84.2 eV and 87.9 eV in figure 3d are corresponding to Au $4f_{7/2}$ and Au $4f_{5/2}$ binding energies [33], proving the formation of metallic gold. What is particularly noteworthy is that the binding energies of S 2p and Mo 3d shift negatively, meanwhile, the binding energy of Au 4f shift positively, as compared to the standard spectrum. This is because the electron of AuNPs transfer to MoS_2 and further form Au-S bond [34-36], indicating strong binding force existed beween the AuNPs and monolayer MoS_2.

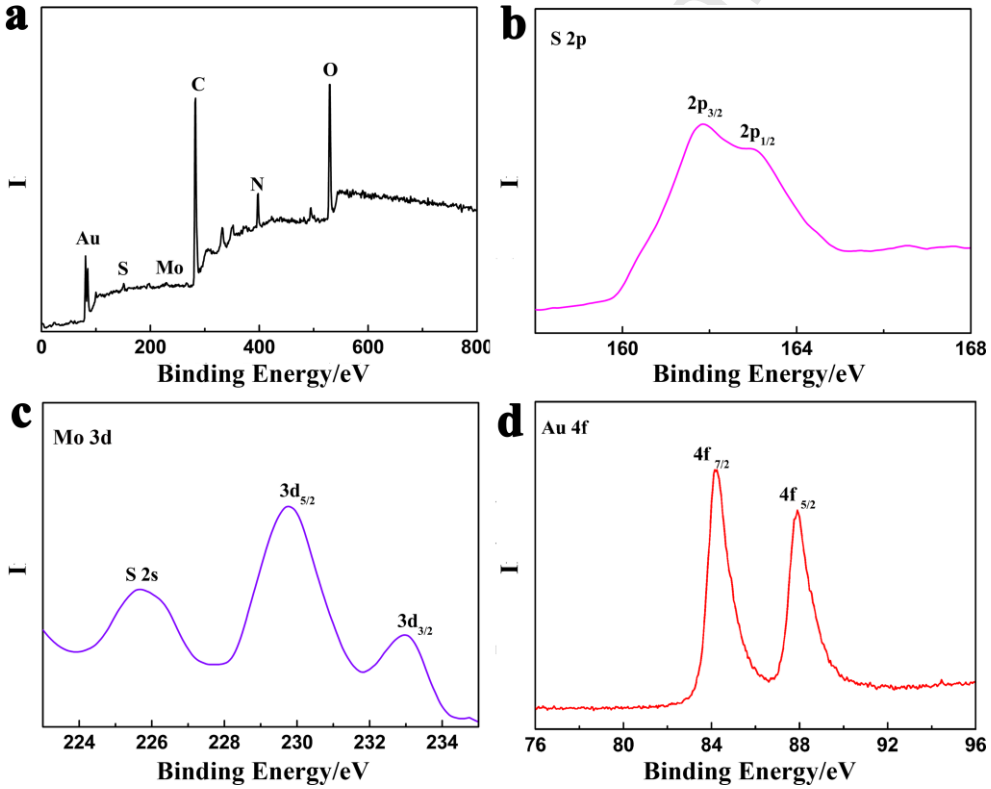

Figure 3 XPS spectra of AuNPs-MoS_2-rGO/PI composite film: (a) survey, (b) S 2p, (c) Mo 3d, (d) Au 4f.

3.2 Electrochemical behavior of ATCh at AChE/AuNPs-MoS_2-rGO/PI electrode

The direct electrochemistry behaviors of the AChE/AuNPs-MoS_2-rGO/PI film electrode towards ATCh were investigated by cyclic voltammetry (CV) with scan rate of 20 mV/s. Figure 4a shows CVs of the AChE/AuNPs-MoS_2-rGO/PI flexible film electrode without ATCh (curve a) and with 90 mg/mL ATCh (curve b) in 0.1 M PBS (pH=7.4). In the absence of ATCh, there was no any redox peak appearing between 0.2 and 0.8 V, which confirms the stability of AChE/AuNPs-MoS_2-rGO/PI film electrode in the potential region. After adding 90 mg/mL ATCh solution, a oxidation peak at 0.49 V was obtained with a significant increase of peak current, indicating the

AChE/AuNPs-MoS_2-rGO/PI film electrode exhibits electrocatalytic activity to ATCh. These results demonstrate the AChE is successfully immobilized on AuNPs-MoS_2-rGO/PI film electrode.

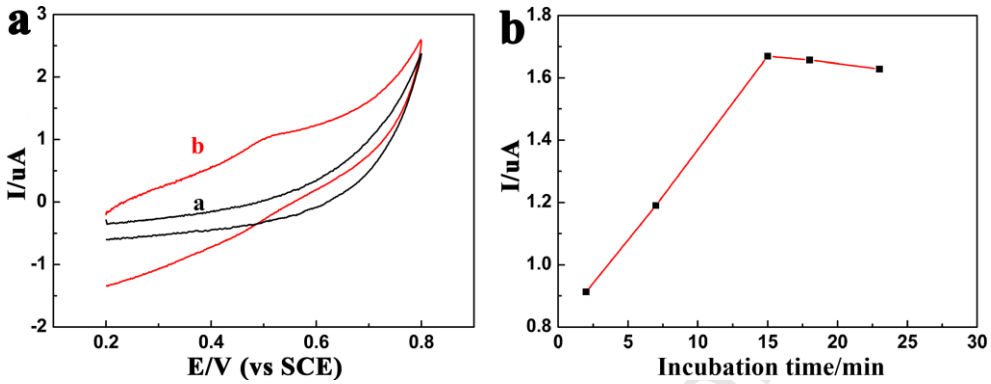

Figure 4 (a) CVs of the AChE/AuNPs-MoS_2-rGO/PI flexible film electrode without ATCh (curve a) and with 90 mg/mL ATCh (curve b) in 0.1 M PBS (pH=7.4). (b) Effects of incubation time on peak current of ATCh at the AChE/AuNPs-MoS_2-rGO/PI electrode. All the scan rate is 20 mV/s.

Before the constructed film biosensor was immersed in the standard solution of paraoxon, the incubation time of AChE/AuNPs-MoS_2-rGO/PI film electrode was measured by DPV. It is find that the oxidation peak currents of ATCh increased with incubation time from 2 to 15 min, and the oxidation peak current reaches maximum at 15 min (figure 4b). After the incubation time exceeded 15 min, the oxidation peak currents decreased with time increase. So the optimum incubation time of AChE/AuNPs-MoS_2-rGO/PI film electrode is 15 min.

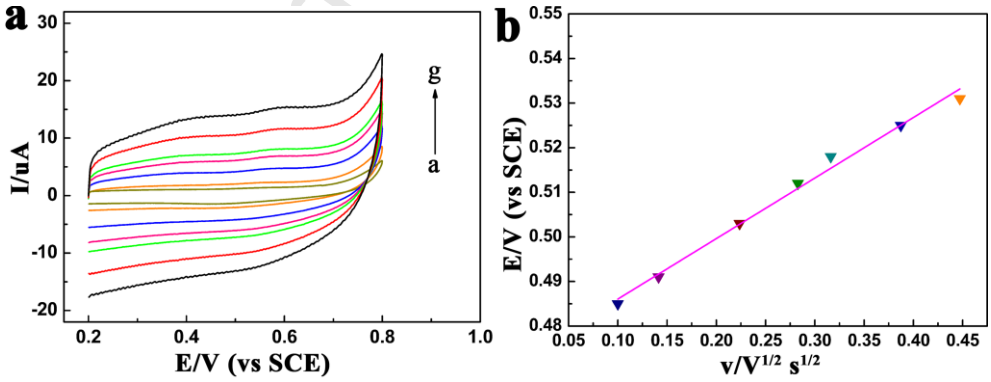

Figure 5 (a) CVs of the AChE/AuNPs-MoS_2-rGO/PI flexible film electrode for 90 mg/mL ATCh in 0.1 M PBS (pH=7.4) at various scan rates (curves a-g): 0.01, 0.02, 0.05, 0.08, 0.10, 0.15, 0.20 V/s. (b) The plots of I_{pa} vs.$v^{1/2}$.

The effect of scan rate on the electrochemical response of ATCh at the AChE/AuNPs-MoS_2-rGO/PI flexible film electrode was also studied by CV. Figure 5 presents CVs of the AChE/AuNPs-MoS_2-rGO/PI flexible film in PBS contained 90 mg/mL ATCh with various scan rates. In the range of 0.01 - 0.20 V/s, the anodic peak

currents increased linearly with the square root of scan rate, which illustrates the electrochemical reaction of ATCh at the AChE/AuNPs-MoS_2-rGO/PI flexible film is a typical diffusion-controlled process [37, 38].

3.3 Application of the AChE/AuNPs-MoS_2-rGO/PI electrode in paraoxon sensing

Accroding to the inhibition mechanism of organophosphorus pesticide to AChE, differential pulse voltammetry (DPV) measurement was performed to evaluate the sensitivity of AChE/AuNPs-MoS_2-rGO/PI film to paraoxon in PBS with 90 mg/mL ATCh. Figure 6a clearly reveals that the peak currents decreased gradually with the paraoxon concentrations ranging from 0.000 to 0.500 μg/mL, indicating paraoxon inhibits intensively the catalytic hydrolysis of AChE. Figure 6b shows the plots of anodic peak currents versus paraoxon concentrations, and the AChE/AuNPs-MoS_2-rGO/PI film displays an extended linear range from 0.005 to 0.150 μg/mL, a sensitivity of 4.44 uA/ug mL^{-1}, a detection limit of 0.0014 μg/mL. Compared with other previous paraoxon enzyme sensors, it can be concluded that the AChE/AuNPs-MoS_2-rGO/PI film sensor has good superiority in terms of detection limit and sensitivity, as shown in Table 1 [13, 39-42].

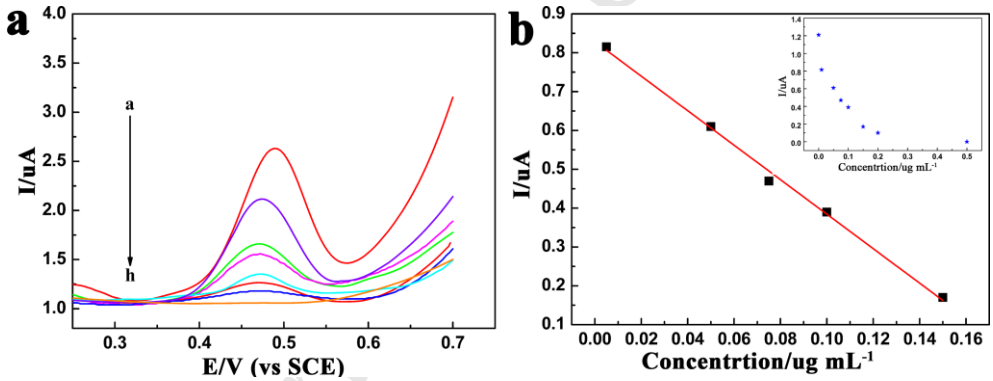

Figure 6 (a) DPV responses of AChE/AuNPs-MoS_2-rGO/PI flexible electrode in PBS within (a-g) or without (h) 90 mg/mL ATCh after inhibition with paraoxon for 15 min. Paraoxon concentration (a)-(g): 0.000, 0.005, 0.050, 0.075, 0.100, 0.150, 0.500 μg/mL. (b) The calibration curves obtained from the DPV responses in (a).

Table 1 The Linear ranges and detection limits of different modified electrodes for the determination of paraoxon.

Electrode	Liner range (μg/mL)	Detection limit(μg/mL)	References
AChE/Au-MoS_2-rGO/PI	0.005-0.150	0.0014	this work
AChE/PANI-MWCNT/GC	0.069-1.350	0.2614	[13]
AChE-SFb/MWNTsc/GCE	0.963- 550.4	0.1376	[39]
AChE/PAMAM-Au/CNTs/GCE	0.001- 0.025	0.0011	[40]
AChE-ChOx/MWCNT/SPE	up to 55.04	0.0138	[41]
AChE/Ni-NTA–cGO/GC	0.0003 -2.75	0.0002	[42]

3.4 Reproducibility and stability

In order to evaluate the reproducibility of AChE/AuNPs-MoS_2-rGO/PI, five film electrodes were investigated in the same conditions towards 0.05 ug/ml paraoxon. The relative standard deviation (RSD) with 4.68% indicates the proposed film electrode possesses good reproducible. As to the long-term stability, the biosensor was stored in refrigerator (4℃) for one week, and the peak current of the same electrode remained 96.0% of its initial value, suggesting the good stability of the AChE/AuNPs-MoS_2-rGO/PI sensor. In this work, the detection of paraoxon is realized by the irreversible inhibition effect, which paraoxon occupies the active site of AChE hydrolyzed ATCh, so the biosensor is used only once.

3.5 Real sample analysis

The application of the proposed AChE/AuNPs-MoS_2-rGO/PI electrode was studied in vegetable sample. Before the test, the vegetable leaves were soaked in 10 mL ultrapure water for 24 h, and then took 1 mL above water into 9 mL PBS contained 90 mg/mL ATCh. The obtained solution is as vegetable water sample. Next, a standard solution of paraoxon was added into vegetable water sample and the detections were performed for three times by DPV method under the same conditions (Table 2). The recoveries keep between 99% and 104% with RSDs of 1.78–4.81%, performing prominent accuracy and reliability. Therefore, the AChE/AuNPs-MoS_2-rGO/PI sensor shows great potential for the analysis of real samples.

Table 2 Determination of paraoxon in vegetable sample.

Added(ng/ml)	Found (ng/ml)	Precision (ng/ml)	Recovery(%)	RSD(%)
10.0	10.4	10.4±0.5	104	4.81
50.0	50.5	50.5±0.9	101	1.78
150.0	149.3	149.3±2.8	99	1.87

4. Conclusions

In this work, we have constructed a paraoxon sensor based on AChE/AuNPs-MoS_2-rGO/PI flexible film. The focus is that AuNPs are reduced on MoS_2-rGO/PI flexible film by means of the photo reduction method. The results of DPV display that AChE modified AuNPs-MoS_2-rGO/PI flexible film electrode has large current response toward ATCh, and shows a linearity range of 0.005–0.150 ug/ml, a sensitivity of 4.44 uA/μg mL^{-1}, a detection limit of 0.0014 μg/ml, good stability and reproducibility for paraoxon. The proposed flexible film biosensor can be used to detect organophosphorus pesticide in real samples.

Acknowledgement

This work is supported by the National Natural Science Foundation of China (Grant Nos. 51372106) and the Dr Fund of Southwest University of Science and Technology (17ZX7131).

References

[1] T. Tian, X. Li, J. Cui, J. Li, Y. Lan, C. Wang, M. Zhang, H. Wang, G. Li, Highly sensitive assay for acetylcholinesterase activity and inhibition based on a specifically reactive photonic nanostructure, ACS Appl. Mater. Interfaces, 6(17) (2014) 15456-15465.

[2] M. Yoonessi, J.R. Gaier, J.A. Peck, M.A. Meador, Controlled direction of electrical and mechanical properties in nickel tethered graphene polyimide nanocomposites using magnetic field, Carbon, 84 (2015) 375-382.

[3] X. Zhang, L. Lu, S. Liu, W. Ye, J. Wu, X. Zhang, Acetylcholinesterase deficiency decreases apoptosis in dopaminergic neurons in the neurotoxin model of Parkinson's disease, Int. J. Biochem. Cell Biol., 45(2) (2013) 265-272.

[4] L.D. Filip Zemek, Eugenie Nepovimova, Vendula Sepsova, Jan Korabecny, Jiri Klimes & Kamil Kuca., Outcomes of Alzheimer's disease therapy with acetylcholinesterase inhibitors and memantine, Expert Opin. Drug Safe., 13 (2014) 759-774.

[5] Q. Zhou, L. Yang, G. Wang, Y. Yang, Acetylcholinesterase biosensor based on SnO_2 nanoparticles-carboxylic graphene-nafion modified electrode for detection of pesticides, Biosens. Bioelectron., 49 (2013) 25-31.

[6] D. Du, X. Ye, J. Cai, J. Liu, A. Zhang, Acetylcholinesterase biosensor design based on carbon nanotube-encapsulated polypyrrole and polyaniline copolymer for amperometric detection of organophosphates, Biosens. Bioelectron., 25(11) (2010) 2503-2508.

[7] D. Song, Y. Wang, X. Lu, Y. Gao, Y. Li, F. Gao, Ag nanoparticles-decorated nitrogen-fluorine co-doped monolayer MoS_2 nanosheet for highly sensitive electrochemical sensing of organophosphorus pesticides, Sensor. Actuat. B- Chem., 267 (2018) 5-13.

[8] X. Lu, L. Tao, D. Song, Y. Li, F. Gao, Bimetallic Pd@Au nanorods based ultrasensitive acetylcholinesterase biosensor for determination of organophosphate pesticides, Sensor. Actuat. B- Chem., 255 (2018) 2575-2581.

[9] D. Song, Y. Li, X. Lu, M. Sun, H. Liu, G. Yu, F. Gao, Palladium-copper nanowires-based biosensor for the ultrasensitive detection of organophosphate pesticides, Anal. Chim. Acta, 982 (2017) 168-175.

[10] C.M. Maroneze, G.P. Dos Santos, V.B. de Moraes, L.P. da Costa, L.T. Kubota, Multifunctional catalytic platform for peroxidase mimicking, enzyme immobilization and biosensing, Biosens. Bioelectron., 77 (2016) 746-751.

[11] R. Sundarmurugasan, M.B. Gumpu, B.L. Ramachandra, N. Nesakumar, S. Sethuraman, U.M. Krishnan, J.B.B. Rayappan, Simultaneous detection of monocrotophos and dichlorvos in orange samples using acetylcholinesterase–zinc oxide modified platinum electrode with linear regression calibration, Sensor. Actuat. B- Chem., 230 (2016) 306-313.

[12] M. Ganesana, G. Istarnboulie, J.L. Marty, T. Noguer, S. Andreescu, Site-specific immobilization of a (His)6-tagged acetylcholinesterase on nickel nanoparticles for highly sensitive toxicity biosensors, Biosens. Bioelectron., 30(1) (2011) 43-48.

[13] I. Cesarino, F.C. Moraes, M.R. Lanza, S.A. Machado, Electrochemical detection of carbamate pesticides in fruit and vegetables with a biosensor based on acetylcholinesterase immobilised on a composite of polyaniline-carbon nanotubes, Food Chem., 135(3) (2012) 873-879.
[14] H. Zhao, X. Ji, B. Wang, N. Wang, X. Li, R. Ni, J. Ren, An ultra-sensitive acetylcholinesterase biosensor based on reduced graphene oxide-Au nanoparticles-beta-cyclodextrin/Prussian blue-chitosan nanocomposites for organophosphorus pesticides detection, Biosens. Bioelectron., 65 (2015) 23-30.
[15] F. Jia, B. Narasimhan, S. Mallapragada, Materials-based strategies for multi-enzyme immobilization and co-localization: A review, Biotechnol. Bioeng., 111(2) (2014) 209-222.
[16] G. Yu, W. Wu, Q. Zhao, X. Wei, Q. Lu, Efficient immobilization of acetylcholinesterase onto amino functionalized carbon nanotubes for the fabrication of high sensitive organophosphorus pesticides biosensors, Biosens. Bioelectron., 68 (2015) 288-294.
[17] Y. Yang, A.M. Asiri, D. Du, Y. Lin, Acetylcholinesterase biosensor based on a gold nanoparticle-polypyrrole-reduced graphene oxide nanocomposite modified electrode for the amperometric detection of organophosphorus pesticides, Analyst, 139(12) (2014) 3055-3060.
[18] C. Xiong, T. Li, T. Zhao, A. Dang, H. Li, X. Ji, W. Jin, S. Jiao, Y. Shang, Y. Zhang, Reduced graphene oxide-carbon nanotube grown on carbon fiber as binder-free electrode for flexible high-performance fiber supercapacitors, Composit. Part B-Eng., 116 (2017) 7-15.
[19] M. Yu, Z. Wang, C. Hou, Z. Wang, C. Liang, C. Zhao, Y. Tong, X. Lu, S. Yang, Nitrogen-doped Co_3O_4 mesoporous nanowire arrays as an additive-free air-cathode for flexible solid-state zinc-air batteries, Adv. Mater., 29(15) (2017).
[20] D. Chen, H. Zhu, T. Liu, In situ thermal preparation of polyimide nanocomposite films containing functionalized graphene sheets, ACS Appl. Mater. Interfaces, 2(12) (2010) 3702-3708.
[21] J. Longun, J.O. Iroh, Nano-graphene/polyimide composites with extremely high rubbery plateau modulus, Carbon, 50(5) (2012) 1823-1832.
[22] M. Yoonessi, Y. Shi, D.A. Scheiman, M. Lebron-Colon, D.M. Tigelaar, R.A. Weiss, M.A. Meador, Graphene polyimide nanocomposites; thermal, mechanical, and high-temperature shape memory effects, ACS Nano, 6(9) (2012) 7644-7655.
[23] K. Wu, K. Du, G. Hu, A novel design concept for fabricating 3D graphene with the assistant of anti-solvent precipitated sulphates and its Li-ion storage properties, J. Mater.Chem. A, 6(8) (2018) 3444-3453.
[24] Y. Jiang, X. Li, S. Yu, L. Jia, X. Zhao, C. Wang, Reduced graphene oxide-modified carbon nanotube/polyimide film supported MoS_2 nanoparticles for electrocatalytic hydrogen evolution, Adv. Funct. Mater., 25(18) (2015) 2693-2700.
[25] L. Jia, X. Sun, Y. Jiang, S. Yu, C. Wang, A novel $MoSe_2$-reduced graphene oxide/polyimide composite film for applications in electrocatalysis and photoelectrocatalysis hydrogen evolution, Adv. Funct. Mater., 25(12) (2015) 1814-1820.

[26] C. Ayala-Orozco, C. Urban, M.W. Knight, A.S. Urban, O. Neumann, S.W. Bishnoi, S. Mukherjee, A.M., Goodman, H. Charron, T. Mitchell, Au nanomatryoshkas as efficient near-infrared photothermal transducers for cancer treatment-benchmarking against nanoshells, ACS Nano, 8 (2014) 6372-6381.
[27] O. Parlak, A. Incel, L. Uzun, A.P.F. Turner, A. Tiwari, Structuring Au nanoparticles on two-dimensional MoS_2 nanosheets for electrochemical glucose biosensors, Biosens. Bioelectron., 89(Pt 1) (2017) 545-550.
[28] J.H. Choi, H. Kim, J.H. Choi, J.W. Choi, B.K. Oh, Signal enhancement of silicon nanowire-based biosensor for detection of matrix metalloproteinase-2 using DNA-Au nanoparticle complexes, ACS Appl. Mater. Interfaces, 5(22) (2013) 12023-12028.
[29] K.F. Mak, C. Lee, J. Hone, J. Shan, T.F. Heinz, Atomically ThinMoS2: A New Direct-Gap Semiconductor, Phy. Rev. Lett., 105(13) (2010).
[30] L. Jia, S. Yu, Y. Jiang, C. Wang, Electrochemical deposition of diluted magnetic semiconductor $ZnMnSe_2$ on reduced graphene oxide/polyimide substrate and its properties, J. Alloy. Compd., 609 (2014) 233-238.
[31] H. Ma, J. Sun, Y. Zhang, C. Bian, S. Xia, T. Zhen, Label-free immunosensor based on one-step electrodeposition of chitosan-gold nanoparticles biocompatible film on Au microelectrode for determination of aflatoxin B1 in maize, Biosens. Bioelectron., 80 (2016) 222-229.
[32] J. Chen, A.A. Jackson, V.M. Rotello, S.R. Nugen, Colorimetric detection of escherichia coli based on the enzyme-induced metallization of gold nanorods, Small, 12(18) (2016) 2469-2475.
[33] L.Y. Wen, F. Xu, B. Xue, Z. Luo, Q. Zhang, B. Bao, S. Su, L. Weng, W. Huang, L. Wang, General synthesis of noble metal (Au, Ag, Pd, Pt) nanocrystal modified MoS_2 nanosheets and the enhanced catalytic activity of Pd-MoS_2 for methanol oxidation, Nanoscale, 6(11) (2014) 5762-5769.
[34] Q. Feng, Y. Du, C. Zhang, Z. Zheng, F. Hu, Z. Wang, C. Wang, Synthesis of the multi-walled carbon nanotubes-COOH/graphene/gold nanoparticles nanocomposite for simple determination of Bilirubin in human blood serum, Sensor. Actuat. B-Chem., 185 (2013) 337-344.
[35] Y. Shi, J. Wang, C. Wang, T.T. Zhai, W.J. Bao, J.J. Xu, X.H. Xia, H.Y. Chen, Hot electron of Au nanorods activates the electrocatalysis of hydrogen evolution on MoS_2 nanosheets, J. Am. Chem. Soc., 137(23) (2015) 7365-7370.
[36] T.S. Sreeprasad, P. Nguyen, N. Kim, V. Berry, Controlled, defect-guided, metal-nanoparticle incorporation onto MoS_2 via chemical and microwave routes: electrical, thermal, and structural properties, Nano Lett., 13(9) (2013) 4434-4441.
[37] X. Ye, Y. Du, D. Lu, C. Wang, Fabrication of beta-cyclodextrin-coated poly (diallyldimethylammonium chloride)-functionalized graphene composite film modified glassy carbon-rotating disk electrode and its application for simultaneous electrochemical determination colorants of sunset yellow and tartrazine, Anal. Chim. Acta, 779 (2013) 22-34.
[38] Y. Jiang, S. Yu, J. Li, L. Jia, C. Wang, Improvement of sensitive $Ni(OH)_2$ nonenzymatic glucose sensor based on carbon nanotube/polyimide membrane, Carbon, 63 (2013) 367-375.

[39] R. Xue, T.-F. Kang, L.-P. Lu, S.-Y. Cheng, Immobilization of acetylcholinesterase via biocompatible interface of silk fibroin for detection of organophosphate and carbamate pesticides, Appl. Surf. Sci., 258(16) (2012) 6040-6045.
[40] Y. Qu, Q. Sun, F. Xiao, G. Shi, L. Jin, Layer-by-Layer self-assembled acetylcholinesterase/PAMAM-Au on CNTs modified electrode for sensing pesticides, Bioelectrochemistry, 77(2) (2010) 139-144.
[41] Y. Lin, F. Lu, J. Wang, Disposable carbon nanotube modified screen-printed biosensor for amperometric detection of organophosphorus pesticides and nerve agents, Electroanalysis, 16(12) (2004) 145-149.
[42] H. Zhang, Z.F. Li, A. Snyder, J. Xie, L.A. Stanciu, Functionalized graphene oxide for the fabrication of paraoxon biosensors, Anal. Chim. Acta, 827 (2014) 86-94.

We declare that we do not have any commercial or associative interest that represents a conflict of interest in connection with the work submitted.

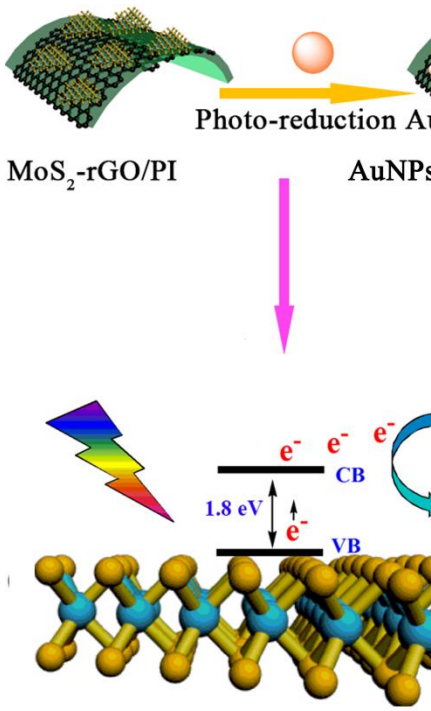

We constructed a paraoxon sensor based on AChE/AuNPs-MoS_2-rGO/PI flexible film. In this work, the rGO/PI film acts as the flexible substrate and AuNPs are reduced by

monolayer MoS_2 under illumination. The AChE modified AuNPs-MoS_2-rGO/PI flexible film biosensor was used to hydrolyze acetylcholine chloride and obtained a large current response at 0.49 V by differential pulse voltammetry. For paraoxon detection, the obtained AChE/AuNPs-

MoS_2-rGO/PI flexible film also shows good sensing property.

An rGO/PI flexible film electrode fabricated without aggregation.

AuNPs reduced on MoS_2-rGO/PI flexible film via optical reduction.

The prepared biosensor displays good response to acetylcholine chloride.

The prepared biosensor exhibits good stability and

reproducibility

to paraoxon.

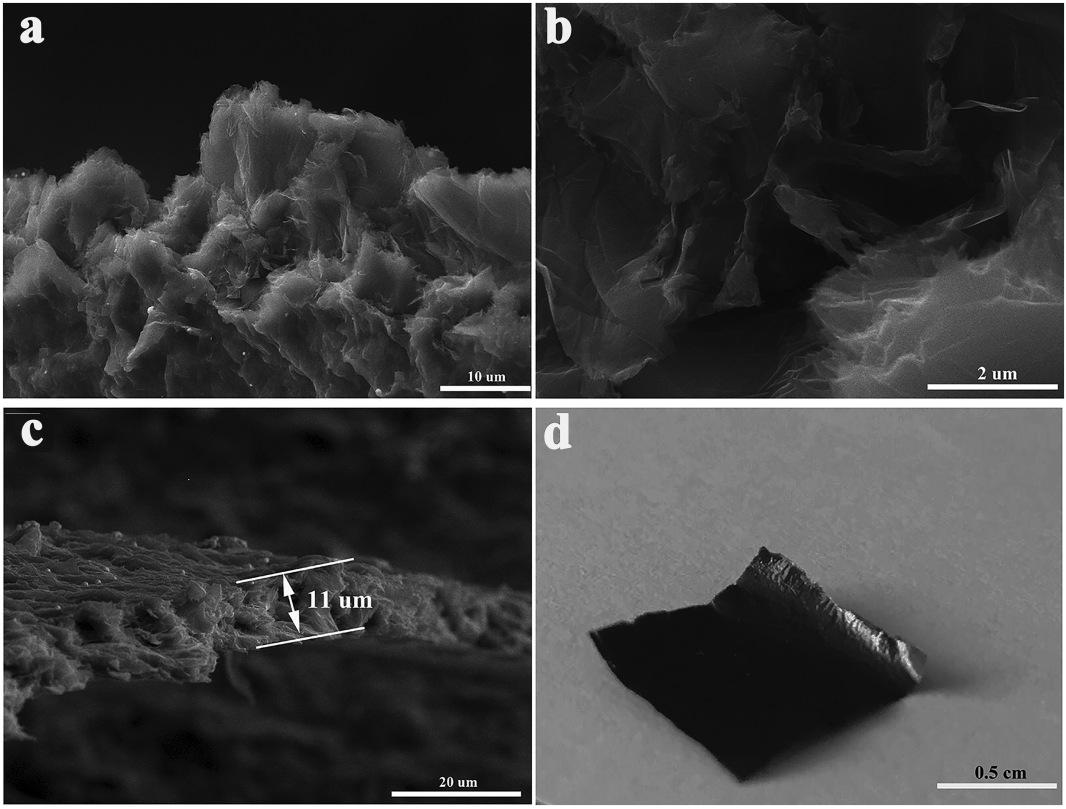

Figure 1

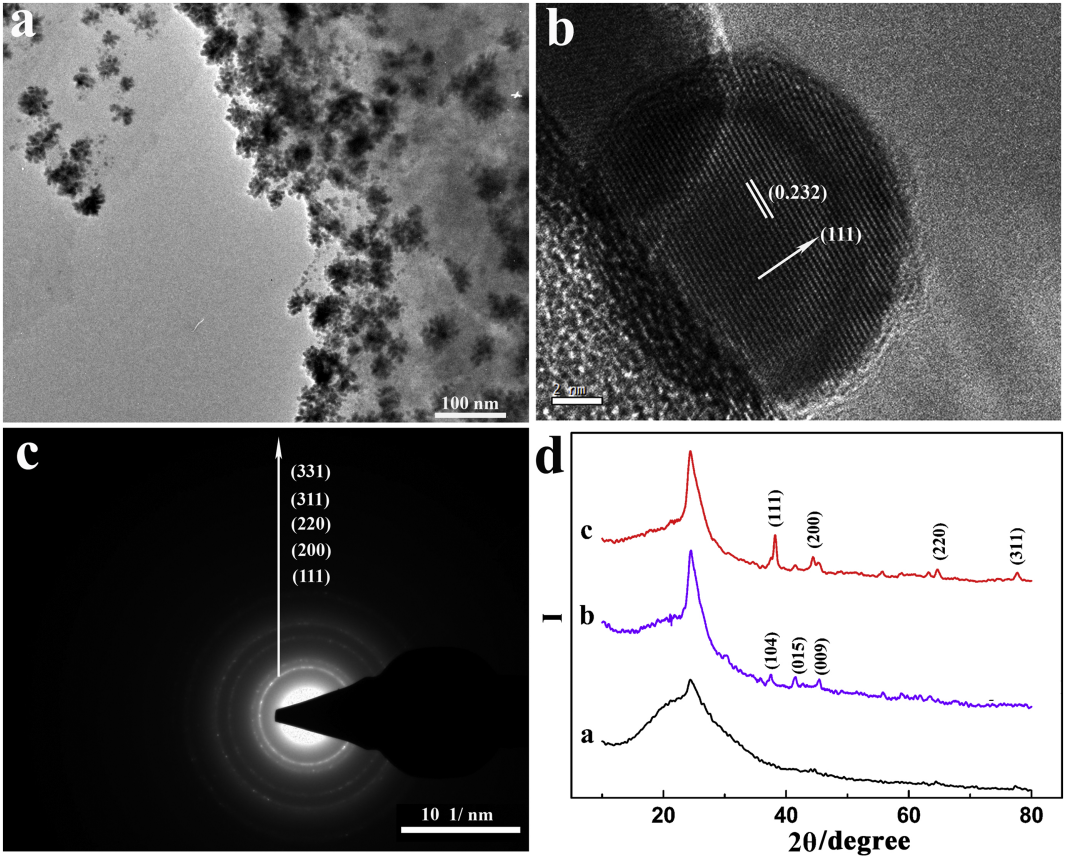
a
100 nm
b
(0.232)
(111)
2 nm
c
(331)
(311)
(220)
(200)
(111)
10 1/ nm
d
c
b
a
I
(111)
(200)
(220)
(311)
(104)
(015)
(009)
20
40
60
80
2θ/degree

Figure 2

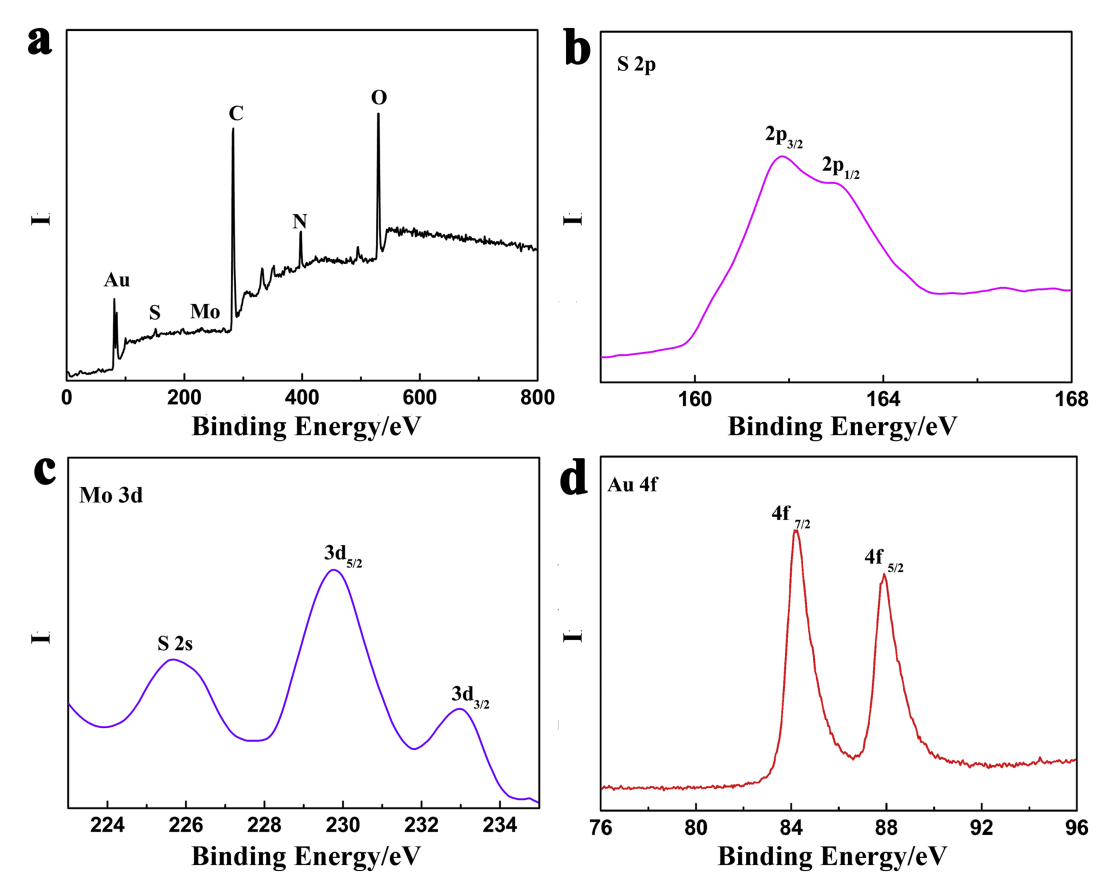
a
I
Au
S
Mo
C
N
O
0
200
400
600
800
Binding Energy/eV
b
S 2p
I
2p3/2
2p1/2
160
164
168
Binding Energy/eV
c
Mo 3d
I
S 2s
3d5/2
3d3/2
224
226
228
230
232
234
Binding Energy/eV
d
Au 4f
I
4f7/2
4f5/2
76
80
84
88
92
96
Binding Energy/eV

Figure 3

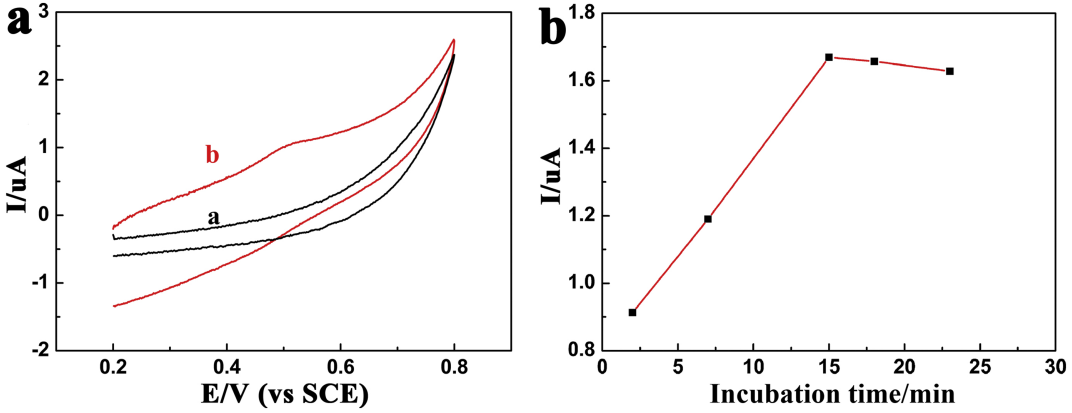

Figure 4

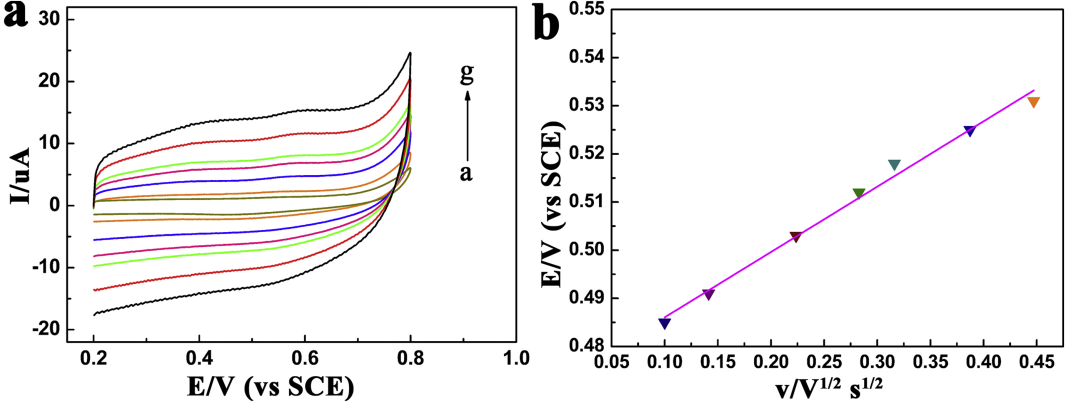

Figure 5

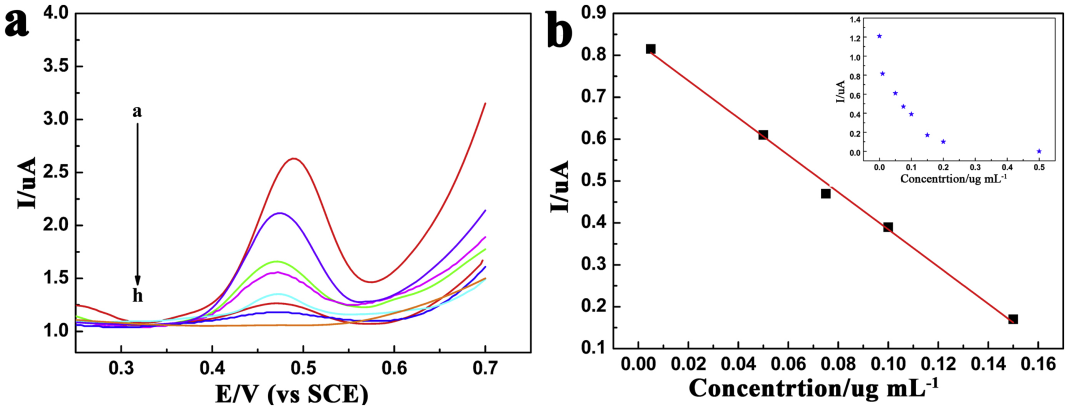
a
I/uA
E/V (vs SCE)
a
h
b
I/uA
Concentrtion/ug mL-1
I/uA
Concentrtion/ug mL-1

Figure 6